Journal of Manufacturing Systems 38 (2016) 107–113

Contents lists available at ScienceDirect

Journal of Manufacturing Systems

journal homepage: www.elsevier.com/locate/jmansys

High-precision and ultrafast UV laser system for next-generation flexible PCB drilling

Kwang-Ryul Kim [a], Jae-Hee Cho [a], Na-Young Lee [a], Hyun-Jin Kim [a], Sung-Hak Cho [b], Hong-Jin Park [c], Byoungdeog Choi [a,*]

[a] Department of Electronic and Electrical Engineering, Sungkyunkwan University, Suwon 440-746, Republic of Korea
[b] Nano Machining Laboratory, Korea Institute of Machinery and Material, 171 Jang-dong, Yuseong-Gu, Daejeon 305-343, Republic of Korea
[c] LTS Co., Ltd, 38-13, Ojeon-dong, Uiwang-si 437-817, Gyeonggi-do, Republic of Korea

ARTICLE INFO

Article history:
Received 23 March 2015
Received in revised form 29 October 2015
Accepted 6 December 2015

Keywords:
High-precision UV laser drilling
Multi-layer FPCB
Automated optical inspection

ABSTRACT

Since conventional mechanical punching technology for Flexible Printed Circuit Board (FPCB) drilling has restricted via-hole size and depth control for multi-layer circuit boards, CO_2 and Ultra Violet (UV) laser drilling technologies have been developed. However, the FPCBs for mobile phones and Personal Digital Assistants (PDAs) require smaller via-hole diameters, since the development of thinner and higher circuit density devices is demanded. Currently, UV laser systems are widely used for FPCB drilling of 75–105 μm diameter via-holes and inspectors performs quality test manually using microscopes. We developed a high-precision UV laser microfabrication system for next-generation FPCB drilling of 15 μm diameter via-holes. The degrees of the precision of the microfabricated via-holes of 15, 35, 50 and 85 μm were mean absolute error rate of 4.4, 2.2, 2.3, and 2.2 which was fully satisfied with industrial inspection specification ±10%. The drilling speed of the system of 2800 via-holes per second at stationary state was achieved. In addition, we applied modified Greedy 2-opt algorithm to find out optimal drilling path which reduced the total time of via-hole fabrication. We successfully reduced the production time by 25% compared with the result obtained in the normal Greedy 2-opt algorithm. Moreover, we designed very accurate inspection method using Canny edge detection and geometric pattern matching algorithms and successfully applied it to the Automated Optical Inspection (AOI) module for the inspections of 15 μm diameter via-hole which was required for the fabrication of high density FPCB.

1. Introduction

The Flexible Printed Circuit Board (FPCB) laser drilling is widely used for small electronic devices, like mobile phones, tablet PCs and PDAs [1–4]. It is also important that tiny via-hole which was fabricated on the FPCB as electronic device kept scaling for high integration. For example, drilling technology through copper foil layer and insulating layer with single laser is required for the rapid growth of the mobile device industry [5–7].

The via-hole drilling capability is varied, depending on the wavelength and characteristics of the processing laser [8,9]. Typically, diameter of via-holes using CO_2 laser fabrication is larger than 50 μm and the UV laser can drill via-hole diameters of less than 35 μm [10,11]. Even though CO_2 laser is widely used in various manufacturing processes, the laser is not appropriate for micromachining applications due to long wavelengths which cause issues about energy coupling, feature size, and plasma [12–14]. Because the FPCB layers consist of copper and polyimide, the absorption of the 10.6 μm wavelength CO_2 laser is less than 10% for basic FPCB materials. On the other hand, the 355 nm wavelength UV laser shows relatively high absorptions for the copper and polyimide materials compare with the one of the CO_2 laser [15]. While CO_2 laser interacts with materials through the photo-thermal effects, like heating and melting, UV laser processes the materials based on the photochemical effects that disconnect molecular binding [16–19]. This photochemical effect can be applied to both copper and polymer materials. Consequently, the UV laser can minimize thermal effect, and achieve more precisely fabricated via-holes than the CO_2 laser [20,21]. Therefore, the UV laser is more suitable for multi-layer FPCB processing [22,23]. Rapidly and precisely drilling is also important as much as tiny via-hole fabrication. Therefore via-hole inspection and optimized algorithms are needed to fabricate a tiny via-hole successfully [24]. In order to reduce the cost and time in the industry, Automated Optical

* Corresponding author. Tel.: +82 31 299 4589; fax: +82 31 299 4589.
E-mail address: bdchoi@skku.edu (B. Choi).

http://dx.doi.org/10.1016/j.jmsy.2015.12.001
0278-6125/

Table 1
UV laser and beam specifications (AWAVE-355).

Items	Specifications
Wavelength (nm)	355
Pulse width (ns)	≤50 (up to 100 kHz)
Average output power (W)	15
Pulse repetition rate (kHz)	Single shot to 300 kHz
Beam roundness	>90%
Beam mode	TEM00

Table 2
Digital galvano scanner specification (intelliSCAN).

Items	Specifications
Typical scan angle	±0.35 rad
Gain error	<5 mrad
Zero offset	<5 mrad
Marking speed	3.0 m/s
Tracking error	0.12 ms
Step response time	0.4 ms

Table 3
Specifications of vision camera and illuminations.

Items	Specifications
Working distance	11 mm
Depth of field	1.72 μm
Focal length	10.0 mm
Spot LED light	Blue
Input	Controller
Ring-guided LED	1 W White

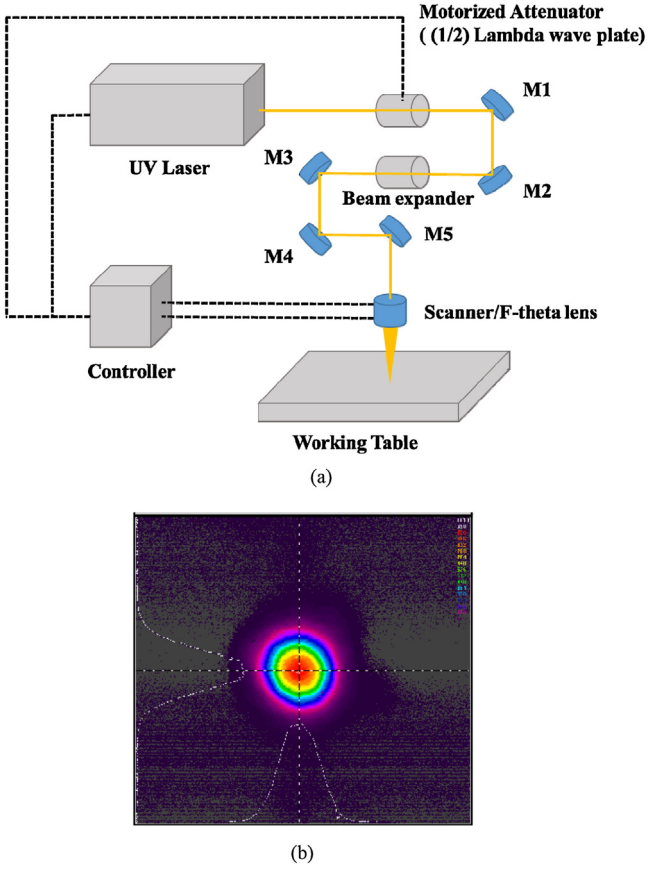

Fig. 1. (a) Schematics of the UV laser drilling system. (b) Intensity profile of the laser beam.

Inspection is an effective way. In this study, tiny via-hole was fabricated on the FPCB rapidly and precisely. The via-hole diameter of 15 μm is most tiny via-hole in current industry. In addition, the Canny edge detection and geometric pattern matching algorithms were used to increase error correction rate and drilling speed [25–28].

2. Experiments

An UV laser, AWAVE-355(Advanced Optowave) was used to fabricate tiny via-holes. The AWAVE-355 laser has average output power of 15 W, and wavelength of 355 nm. It also shows very nice beam quality in beam roundness more than 90%. The laser and beam specifications of the AWAVE are presented in Table 1. The laser beam is delivered through an attenuator, mirrors, and it is magnified through a beam expander. The energy of the UV laser is controlled by the motorized attenuator. The FPCB fabrication was processed through UV scanner on a precise stage table. The schematics of the laser beam delivery system are represented in Fig. 1(a). The focal length of the f-theta lens was 55 mm and beam spot size was 8 μm. We radiated single pulse of UV laser on the testing copper plate and measured the diameter of the spot under the microscope. In addition, the beam profile of the UV laser is showed in Fig. 1(b). This profile demonstrates that the intensity of the laser is symmetrical in the vertical and horizontal dimensions. Typical layers of the FPCB for mobile phone are illustrated in Fig. 2(a). It is composed of three layers: the upper layer is 12 μm copper foil, the middle layer is 12 μm of polyimide, and the lower layer is 12 μm copper foil again. The via-hole was designed to be fabricated through the first and second layers. It is called blind via hole. The geometry of typical via-hole and definitions of the blind via-hole structure for AOI process are shown in Fig. 2(b). Because radiated laser energy is decreased near the side wall boundary, diameter of the upper layer is always larger than that of the lower layer. A digital galvano scanner intelliSCAN (SCANLAB), which is used for patterning of the laser microfabrication, is installed at the end of the beam delivery path. The specification of the digital galvano scanner is presented in Table 2. We installed intelliSCAN, an advanced digital scanner, on the system because it is more accurate and stable from the thermal drift effect compared with the conventional analog scanner. The illumination and vision camera with proper lenses are very important components because the system requires inspecting the defected via-holes visually. We used a spot LED and vision camera with ring-guide LED. The specification of the vision camera and illuminations are shown in Table 3.

Researchers began to use the Greedy 2-opt algorithm to find out the optimal travel path and reduce the travelling time [29,30]. Flow chart for the Greedy 2-opt and modified Greedy 2-opt algorithms were well presented [31]. The main improvement from the Greedy 2-opt to modified Greedy 2-opt algorithms is “getting rid of the crossings”. In this study, we applied the modified Greedy 2-opt algorithm to figure out the optimal drilling path and reduce the processing time.

Normally defections of the drilled via-holes are classified under five categories which are resin residue, shifted, over processed, missing hole, and eccentricity. The shapes of the normal and defective holes are shown in Fig. 3. The ‘resin residue’ exists as a remainder on bottom layer after the via-hole fabrication. The ‘shifted’ or ‘twisted hole’ is a shift processed hole because laser is moved during fabrication. The ‘over processed’ is fabrication through the third layer. The ‘missing hole’ is non-processed or missing, and the ‘eccentricity’ is dislocation of the via-hole center of the upper hole and bottom. The detailed explanation of the defections

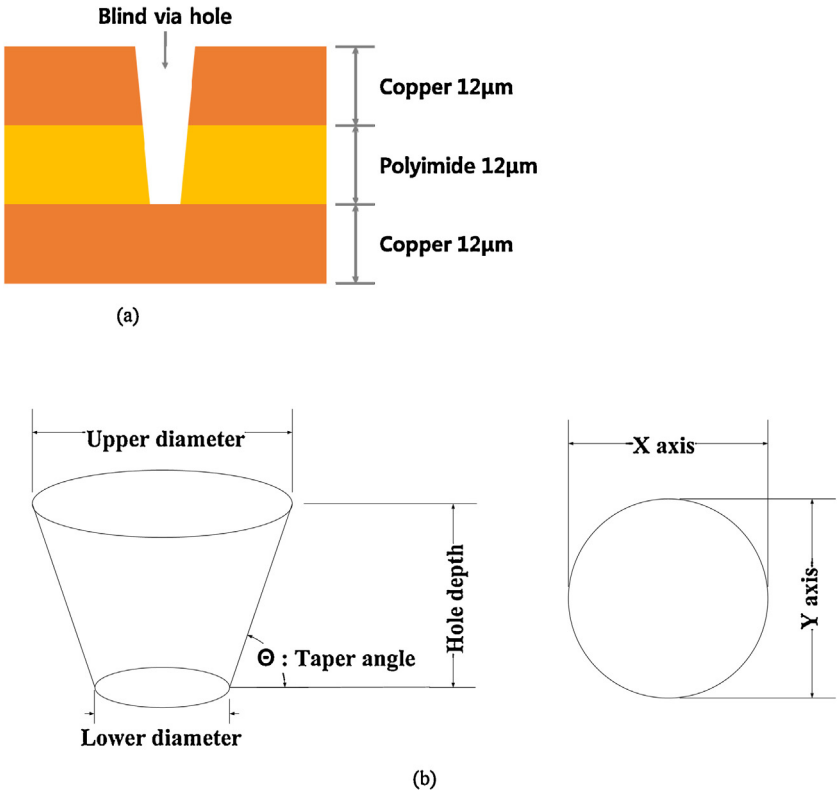

Fig. 2. (a) Cross-sectional view of FPCB layers and blind via-hole. (b) Definitions of blind via-hole structure for AOI process.

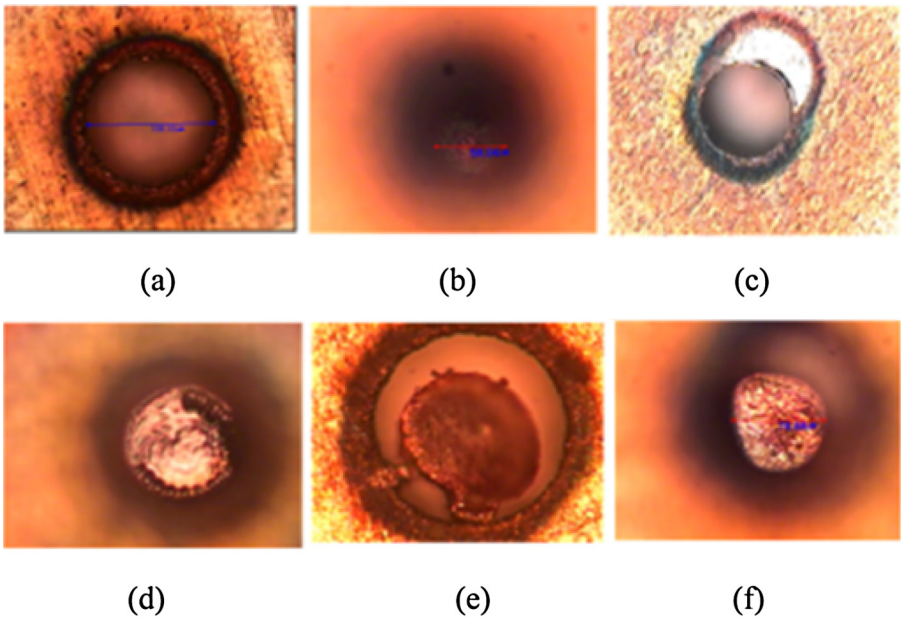

Fig. 3. Classifications of defected via-holes. Camera is focused on the upper layer of FPCB.
(a) Normal hole (b) Resin residue (c) Shifted (d) over processed (e) Missing hole (f) Eccentricity.

and other required inspection standard like mean absolute error rate of the via hole size on the top layer, roundness, and required taper angle are presented in Table 4.

The Canny edge detection algorithm was used to develop accurate AOI process. The Canny edge detection algorithm is an image processing algorithm that finds the edge of an object. We used this algorithm to categorize laser-processed holes as well-fabricated holes or defective holes. A flowchart of the algorithm is shown in Fig. 4. In this algorithm, input image *A* is filtered using a Gaussian

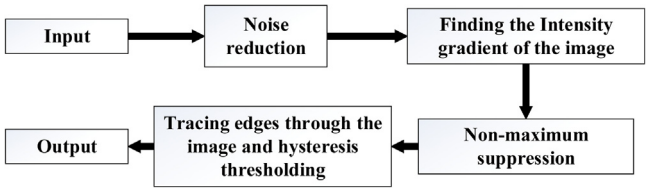

Fig. 4. Canny edge detection algorithm used in automated optical inspection process for via-hole in FPCB.

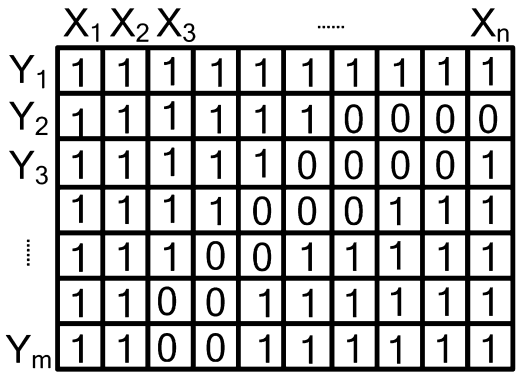

Fig. 5. An example of output image after running the canny edge detection algorithm in 2nd quadrant. Input image is converted to bit '0' and '1', which indicate selected edge pixel and discarded pixel, respectively.

Table 4
The criterion of defect inspection.

Inspection items	Status	Inspection standard
Holes missing	Non-processed or missing	Check through microscope
Hole size	Supervising hole sizes	Top: specification ±10% Bottom: 70% over than spec.
Eccentricity	Dislocation of upper hole and bottom hole.	Clean
Over process	Hole over processed through the bottom surface	Clean
Resin residue	Resin residue in bottom hole	Clean
Twisted hole	Shift processed of holes	Clean
Roundness	Roundness of hole shape	>90%
Taper angle		>70°

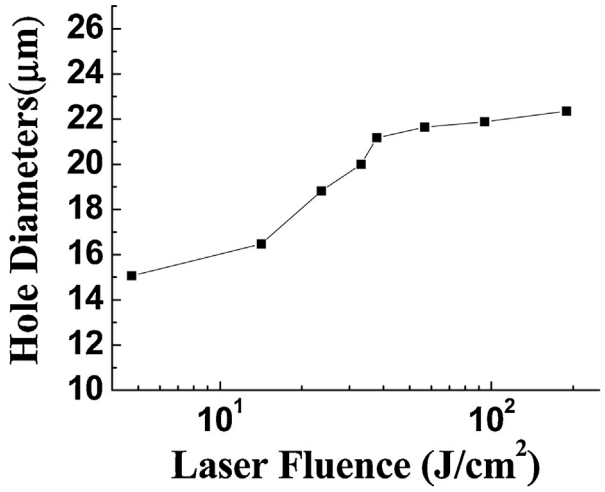

(a)

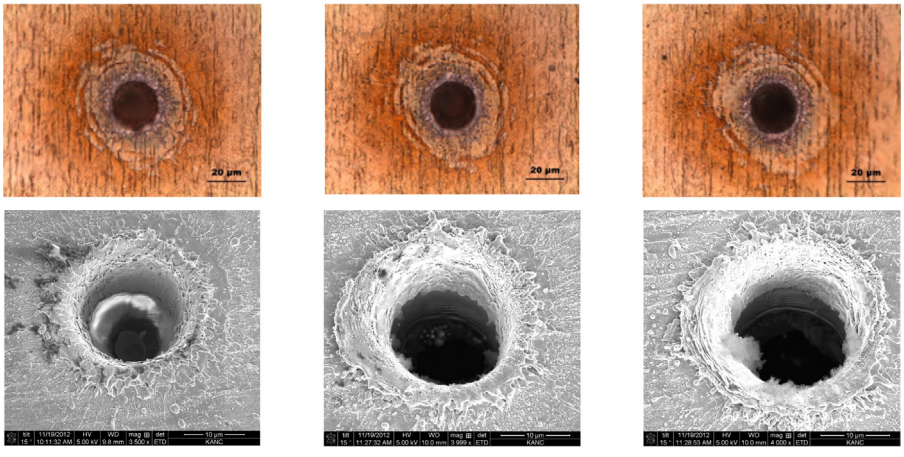

(b) (c) (d)

Fig. 6. (a) Experimental results of the relationship between laser fluence on logarithmic scale and hole diameters (b) Microscopic and SEM pictures of the drilling holes according to the laser power of 0.48 W. (c) 0.67 W. (d) 1.14 W.

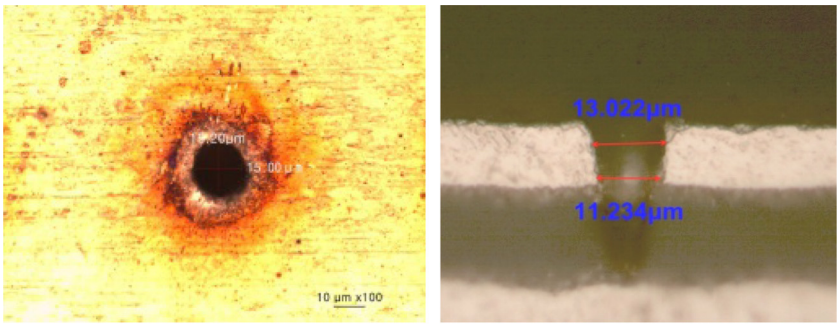

Fig. 7. (a) Microscopic image of the 15 μm via hole on upper layer (b) Cross-sectional view.

matrix to reduce the noise. This is done through 2-dimension convolution as follows [32].

$$B = \frac{1}{159}\begin{bmatrix} 2 & 4 & 5 & 4 & 2 \\ 4 & 9 & 12 & 9 & 4 \\ 5 & 12 & 15 & 12 & 5 \\ 4 & 9 & 12 & 9 & 4 \\ 2 & 4 & 5 & 4 & 2 \end{bmatrix} \times A \tag{1}$$

After this step, the Gaussian filtered image B is differentiated through x and y-axis by convolution with sobel mask. Matrixes used in these steps are expressed as follows [32,33].

$$G_x = \begin{bmatrix} -1 & 0 & 1 \\ -2 & 0 & 2 \\ -1 & 0 & 1 \end{bmatrix} \times B, \quad G_y = \begin{bmatrix} 1 & 2 & 1 \\ 0 & 0 & 0 \\ -1 & -2 & -1 \end{bmatrix} \times B \tag{2}$$

where the G_x and G_y are magnitude of each pixel on x and y-axis. The input image has magnitude G and direction θ after convolution. The equations for these values are shown as below.

$$G = \sqrt{G_x^2 + G_y^2}, \quad \theta = \tan^{-1}\left(\frac{|G_y|}{|G_x|}\right) \tag{3}$$

Then we must choose the pixel which has biggest magnitude among the adjacent pixels and link them together. These lines become the edge of the input image. The edge of the object will be shown in white and this will be zero bit, and the other pixels are expressed with a 1 bit after being processed by the edge detection algorithm. An example of the output image after running the Canny edge detection algorithm is expressed in Fig. 5. Only 2nd quadrant part of the output image is presented in the figure. The pattern matching algorithm is an image comparison algorithm and performed after Canny edge detection. The image that is processed by the Canny edge detection algorithm is used as inputs. It analyzes the pixels of the input image, and compares them with those of the other image, to calculate the pixel matching percentage, R. Equation is shown below.

$$R = \frac{\sum\sum\{[x_{nk}, y_{mk}] + [x_{nl}, y_{ml}]\}}{nm - \sum\sum[x_{ik}, y_{jk}]} \tag{4}$$

where n and m are the number of pixels in x and y-axes. The suffix k indicates the reference input image and l indicates the image of the comparison target. Therefore, x_{nk} means the nth pixel on the x-axis of the reference (k) input image, and y_{ml} is the mth pixel on the y-axis of the comparison (l) target image. The denominator in Eq. (4) is the number of white pixels, which indicate edges, and the numerator is the number of white pixels after comparing the target image with the reference image. This algorithm analyzes the difference of each input image by comparing the location and shape of the hole, which is expressed in white pixels.

3. Results and discussions

The fabrication is processed using an AWAVE-355 UV laser and digital scanner. The experimental results of the relationship between laser fluence and hole-diameters were presented in Fig. 6(a). The beam spot size of the UV laser was 8 μm and pulse width was 10 ns. A single pulse percussion drilling method was applied to implement fast drilling speed. The diameters of the via-holes were logarithmically increased according to laser fluence. Moreover, microscopic and SEM images of the drilling holes according to the laser power of 0.48 W, 0.67 W, and 1.14 W were shown in Fig. 6(b). The diameters for each laser energy were 18.8, 20.0, 21.6 μm. The average roundness of the 15 μm via-hole was 95% which was satisfied with the industrial inspection standard when we calculated the average value of the 100 sample holes. Microscopic image of the 15 μm via-hole on upper layer and cross-sectional view were also presented in Fig. 7. The average taper angle was 84 degree with same samples which was also satisfied with the industrial inspection standard. The measured diameters and mean absolute error rates of the fabricated via holes are shown in Fig. 8. Designated via-hole diameters on upper layer were 15, 35, 50 and 85 μm and averaged mean absolute error rate of fabricated via-hole diameters are 4.4, 2.2, 2.3, and 2.2%. Mean absolute error rate is average of the absolute diameter difference values between target hole and actual fabricated hole. All these data are satisfied because the specification for industrial inspection standard is ±10%. Beside the drilling speed is 40% faster than UV laser drilling system, Electro Scientific Industries 5330 (ESI 5330), which has drilling speed of 2000 holes per second.

We drilled 32,604 via-holes and checked out the processing time. When we applied the Greedy 2-opt algorithm, it took 162 s. On

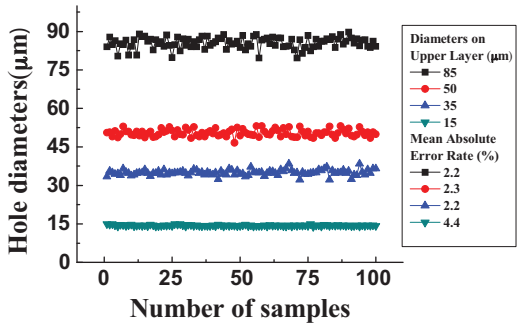

Fig. 8. Mean absolute error rate of the fabricated via hole diameters of 15, 35, 50, and 85 μm.

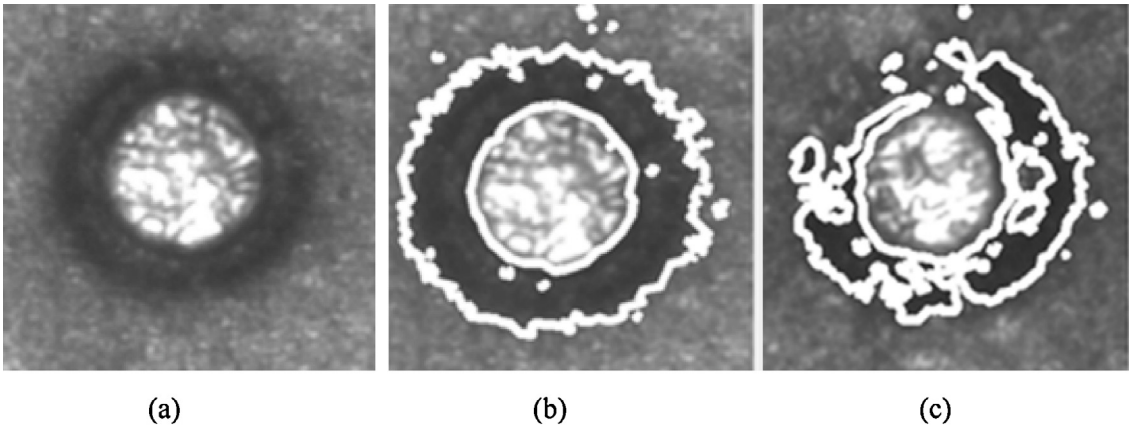

Fig. 9. (a) Target via-hole image (b) Edge detection image after applying the Canny edge detection algorithm for normal hole and (c) Defected hole.

the other hand, it took 122 s for processing time applying the modified Greedy 2-opt algorithm. This means 25% system performance improvements. We successfully applied the modified Greedy 2-opt algorithm for UV-laser drilling optimal path.

The via-hole images through vision camera under the conditions of three different light sources which are ring guided light, axial illumination and ring guided illumination with axial light were tested. The incidence angle of the ring guide light is about 15° and it induces distraction of the light, and causes a decline in image quality. An axial illumination minimizes the distracted light, because it is perpendicularly installed on the FPCB, with an incidence angle of 0°. The image with using both axial illumination and the ring guide light is the most vivid image, and is most suitable to apply for the AOI process. A normal hole shows good roundness after the algorithm, while a defective hole shows an output image with a rough edge. With each output image, we applied the geometric pattern matching algorithm. The results of the AOI process are presented in Fig. 9(a)–(c). The figure shows the via-hole edge detection image of the target hole. After applying the Canny edge detection algorithm for normal via-hole and defected one. We drilled 200 via-hole samples and intentionally created 5 defected holes for testing of the AOI process. The matching percentages at each via-hole sample after AOI process for diameter of 50 μm and 15 μm were presented in Fig. 10. Normal holes that were fabricated properly show a matching percentage, *R*, of more than 90%. Defective holes, which have abnormal shapes, have a matching percentage lower than 75%. Points inside the ellipse means defected via-holes. We successfully tested the AOI process through this experiment.

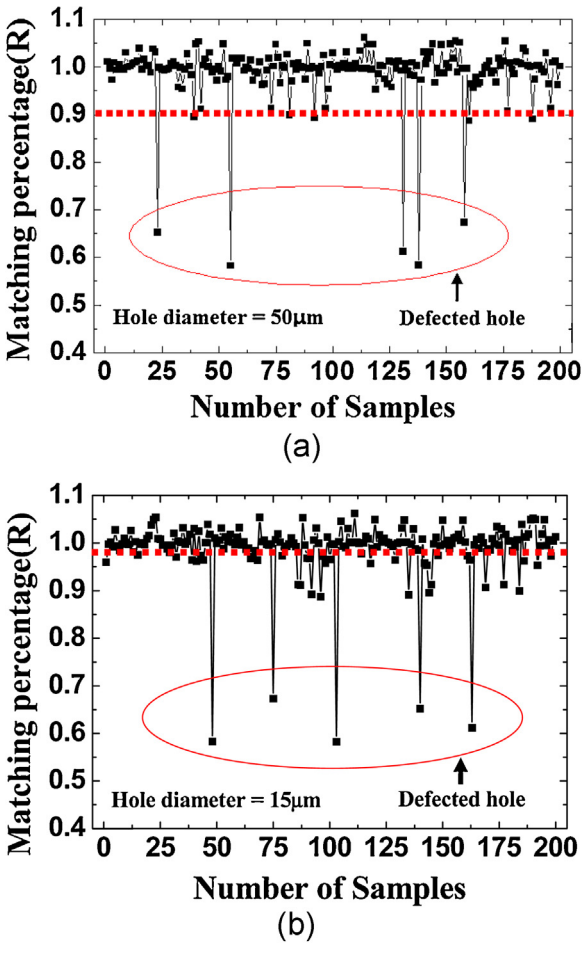

Fig. 10. Matching percentages at each via-hole sample after AOI process for diameter of (a) 50 μm (b) 15 μm. Points inside the ellipse means defected via-holes.

4. Conclusions

The fabrication of tiny holes on FPCB have become significant issue in the mobile device industry, since the development of thinner and higher circuit density devices is in demand. In this study, tiny via-hole was successfully fabricated by using UV laser system with high speed drilling. The drilling speed of 2800 holes per second is faster than current industrial standard; other one has speed of 2000 holes per second. In addition, we achieved via-hole diameter of 15 μm which shows 95% of roundness and 84° of taper angle. Microfabricated via holes has diameter of 15, 35, 50 and 85 μm using the UV laser system and obtained averaged mean absolute error rate less than current industry standard specification. Moreover, the modified Greedy 2-opt algorithm was applied to UV-laser drilling to find out optimal drilling path which reduced the total time of hole fabrication. We minimized the number of path intersections in the applied version, compared to the result obtained in the normal Greedy 2-opt algorithm. As a result, we successfully reduced the production time by 25%. In addition, the Canny edge detection algorithm and pattern matching algorithm were used to detect the defective micro via-holes automatically. The result of the pattern matching algorithm showed a lower matching percentage in defective via holes. We detected defective via-holes using the pattern matching and Canny edge detection algorithms. In this manner, we successfully applied the AOI process using the geometric pattern matching algorithm rather than finding the defective holes manually by visual inspection as currently done in the laser drilling industry.

Acknowledgements

This research was supported by the Ministry of Trade, Industry & Energy (10033701).

References

[1] Gower MC. Industrial applications of laser micromachining. Opt Express 2000;7:56–67.
[2] Yung KC, Zeng DW, Yue TM. XPS investigation of Upilex-S polyimide ablated by 355 nm Nd: YAG laser irradiation. Appl Surf Sci 2001;173:193–202.
[3] Holden HT. The developing technologies of integrated optical waveguides in printed circuits. Circuit World 2003;29:42–50.
[4] Yung WK, Liu JS, Man HC. Experimental investigation of 355 nm Nd: YAG laser ablation of RCC^{R} in PCB. Circuit World 1999;25:13–7.
[5] Schmidt M, Eber G. The future of lasers in electronics. In: Proceedings of ICALEO. 2003.
[6] Meier DJ, Schmidt SH. PCB laser technology for Rigid and Flex HDI—via formation, structuring, routing. CIRCUITREE-CAMPBELL 2002;15:22.
[7] Dunsky C. High-speed microvia formation with UV solid-state lasers. Proc IEEE 2002;90:1670–80.
[8] Gan EKW, Zheng HY, Lim GC. Laser drilling of micro-vias in PCB substrates. In: Proceedings of 3rd electronics packaging technology conference 2000. 2000. p. 321–6.
[9] Kim KR, Kim TH, Park HA, Kim SY, Cho SH, Yi J, Choi BD. UV laser direct texturing for high efficiency multicrystalline silicon solar cell. Appl Surf Sci 2013;264:404–9.
[10] Huske M. Burr and stress-free cutting of flexible printed circuits. OnBoard Technol 2006;6:18–21.
[11] Zhang C, Salama IA, Quick NR, Kar A. Modelling of microvia drilling with a Nd: YAG laser. J Phys D: Appl Phys 2006;39:3910.
[12] Chang TC, Molian PA. Excimer pulsed laser ablation of polymers in air and liquids for micromachining application. J Manuf Processes 1999;1:1–17.
[13] Sheng P, Cal L. Predictive process planning for laser cutting. J Manuf Syst 1998;17:2.
[14] Paul R, Anand Sam. Process energy analysis and optimization in selective laser sintering. J Manuf Syst 2012;31:429–37.
[15] Cable A. Improvement in high speed laser microvia formation using solid state Nd: YAG UV lasers. In: IPC Works' 97; 1997.
[16] Dabby FW, Paek UC. High-intensity laser-induced vaporization and explosion of solid material. IEEE J Quantum Electron 1972;8:106–11.
[17] Bäuerle D, Himmelbauer M, Arenholz E. Pulsed laser ablation of polyimide: fundamental aspects. J Photochem Photobiol A: Chem 1997;106.1:27–30.
[18] Srinivasan R, Hall RR, Loehle WD, Wilson WD, Allbee DC. Chemical transformations of the polyimide Kapton brought about by ultraviolet laser radiation. J Appl Phys 1995;78:4881–7.
[19] Yung KC, Zeng DW, Yue TM. High repetition rate effect on the chemical characteristics and composition of Upilex-S polyimide ablated by a UV Nd:YAG laser. Surf Coat Technol 2002;160:1–6.
[20] Luk'yanchuk B, Bityurin N, Himmelbauer M, Arnold N. UV-laser ablation of polyimide: from long to ultra-short laser pulses. Nucl Instrum Methods Phys Res, Sect B: Beam Interact Mater Atoms 1997;122:347–55.
[21] Aguilar CA, Lu Y, Mao S, Chen S. Direct micro-patterning of biodegradable polymers using ultraviolet and femtosecond lasers. Biomaterials 2005;26:7642–9.
[22] Oh JY, Shin BS. Photothermal and photochemical investigation on laser ablation of the polyimide by 355 nm UV laser processing. J Korean Soc Precis Eng 2007;24(4):147.
[23] Oh JY, Shin BS. A study on laser ablation of copper thin foil by 355 nm UV laser processing. J Korean Soc Precis Eng 2007;24:147–52.
[24] Moganti M, Ercal F, Dagli CH, Tsunekawa S, Automatic PCB. inspection algorithms: a survey. Comput Vis Image Understanding 1996;63:287.
[25] Sherif SU, Jawahar N, Balamurali M. Sequential optimization approach for nesting and cutting sequence in laser cutting. J Manuf Syst 2014;33:624–38.
[26] Liu X. In situ metrology system for micro-milling machine. J Manuf Syst 2012;31:15–21.
[27] Canny J. A computational approach to edge detection. IEEE Trans Pattern Anal Mach Intell 1986;6:679–98.
[28] Ding L, Goshtasby A. On the canny edge detector. Pattern Recognit 2001;34:721–5.
[29] Černý V. Thermodynamical approach to the traveling salesman problem: an efficient simulation algorithm. J Optim Theory Appl 1985;45:41–51.
[30] Tropp JA, Gilbert AC, Strauss MJ. Algorithms for simultaneous sparse approximation. Part I: Greedy pursuit. Signal Process 2006;86:572–88.
[31] Kim B, Shim J, Zhang M. Comparison of TSP algorithms. In: Project for models in facilities planning and materials handling; 1998.
[32] Shapiro LG, Stockman GC. Computer vision: theory and applications. New Jersey: Prentice Hall; 2001.
[33] Engel K, Hadwiger M, Kniss JM, Rezk SC. Real-time volume graphics. 1st ed. A K Peters; 2006.